ELSEVIER

Journal of Neuroscience Methods 94 (2000) 205–215

JOURNAL OF NEUROSCIENCE METHODS

www.elsevier.com/locate/jneumeth

A method for measuring colocalization of presynaptic markers with anatomically labeled axons using double label immunofluorescence and confocal microscopy

Michael A. Silver, Michael P. Stryker *

Department of Physiology, Room S-762, W.M. Keck Center for Integrative Neuroscience and Neuroscience Graduate Program, University of California, 513 Parnassus Avenue, San Francisco, CA 94143-0444, USA

Received 8 April 1999; received in revised form 4 August 1999; accepted 6 September 1999

Abstract

Information concerning the location and distribution of presynaptic neurotransmitter release sites within anatomically labeled axons would be of value for a large number of studies in functional anatomy, development, and plasticity. Here we report a method for localizing presynaptic sites within identified arbors of interest using anterograde anatomical tracer injections to label axonal projections and synaptic vesicle protein (SVP) antibodies to label presumptive presynaptic terminals. The axons and presynaptic sites are independently visualized with double label immunofluorescence and confocal microscopy. Stacks of images representing adjacent focal planes are collected, and image processing techniques are applied to identify the location of each axonal branch segment and each cluster of SVP label in three-dimensional space. Segmentation of the SVP label into distinct pixel clusters in three-dimensional space, followed by colocalization of these clusters with the labeled axons (object-based analysis), yields much more reliable and sensitive measures of colocalization than a simple determination of the number (or summed intensities) of colocalized pixels in a single optical section (pixel-based analysis). The method has been extended to measure the colocalization of antigens that are not located at the presynaptic terminal with a labeled population of axons.

Keywords: Colocalization; Confocal microscope; Immunofluorescence; Synaptic vesicle protein; Presynaptic terminal; Synaptophysin; Lateral geniculate nucleus; Visual cortex

1. Introduction

Studies using light microscopy to investigate the morphology of single arbors have provided important information about basic neuroanatomy, development, and plasticity (Humphrey et al., 1985; Antonini and Stryker, 1993b). Although anatomical identification of presynaptic terminals of labeled axons would be useful for addressing a wide range of neurobiological questions, this can be difficult to achieve at the light microscope level. While many presynaptic terminals in the mature brain are associated with clear swellings of the axon, such synaptic boutons are often not apparent earlier in development or during periods of plasticity (LeVay and Stryker, 1979; Antonini and Stryker, 1993a). More accurate measurements of the location and distribution of presynaptic neurotransmitter release sites within axons of interest is possible at the electron microscope level (Freund et al., 1985; Hamos et al., 1987; Friedlander et al., 1991). However, electron microscopic studies can be very time- and labor-intensive, especially when three-dimensional reconstructions of synapses from serial sections are required. As a result, the number of axons in an electron microscopic study is typically low, and often only a portion of a given axonal arbor is analyzed. Furthermore, the amount of time required makes studies of development or plasticity, for which measurements must be made at multiple time points, very difficult.

Recently, the availability of synaptic vesicle protein (SVP) antibodies has allowed the visualization of presumptive presynaptic terminals at the light microscope level using standard immunohistochemical techniques

* Corresponding author.

0165-0270/00/$ - see front matter
PII: S0165-0270(99)00145-4

(Hooper et al., 1980; Matthew et al., 1981; Wiedenmann and Franke, 1985; Südhof, 1995). Colocalization of these immunolabeled presynaptic sites with label from anatomical tracer molecules provides a means of identifying the location and distribution of SVP label in axons of interest that have been labeled using standard tract-tracing methods (Pinches and Cline, 1998). Since SVP antibodies label all of the presynaptic sites in a tissue section, a method is required for visualizing only the small fraction of total presynaptic sites that are located within the labeled axons. This can be accomplished by generating thin optical sections of double-labeled immunofluorescent tissue with a confocal microscope.

Although confocal microscopy can be effective at removing a substantial amount of signal generated by labeled structures located above and below the focal plane of interest, the top and bottom surfaces of an optical section are not absolute. Every fluorescently labeled structure has a point spread function that describes how the fluorescent signal from the structure decreases as it is moved away from the center of the optical section (out of the focal plane). The shape of this function will depend in part on the thickness of the optical section, which is determined in turn by the optics and aperture size of the confocal microscope (Carrington et al., 1990). Fluorescently labeled structures above and below the focal plane will contribute some out of focus scatter to any given optical section.

In the case of colocalization of presynaptic sites with labeled axons, such scatter may lead to false positive colocalization of a labeled axon branch with a presynaptic site that is actually located within an unlabeled axon that is immediately above or below the labeled axon. This false positive artifact may be substantial even if the amount of out of focus contribution from each presynaptic site is extremely small, because only a small percentage of the total axons in a given field is likely to contain the anatomical tracer. Therefore, the number of presynaptic sites within unlabeled axons will be much larger than the number of sites within labeled axons. If the amount of colocalization were quantified using a pixel-based analysis, that is, by simply counting the number of apparently colocalized pixels (or summing their intensities) in single optical sections, the false positive artifact could contribute substantially to, or even dominate, the colocalization measurement.

To address the problem of false positive colocalization artifact, we have used image thresholding and segmentation techniques to separate the clusters of SVP labeling into distinct objects whose three-dimensional positions can be accurately determined in a stack of serial optical sections (object-based analysis). This method allows much more precise measurement of colocalization of individual presynaptic sites with the labeled axons of interest than would be possible using measurements from a pixel-based analysis of a single optical section. This object-based analysis is also useful for determining whether a given antigen is colocalized with a population of labeled axons even if the antigen is not expressed at the presynaptic terminal.

2. Methods

2.1. Confocal microscope calibration

The point spread function of the Biorad MRC600 confocal microscope used in these experiments was derived using 0.2 μm diameter fluorescent beads (supplied by Biorad (Hercules, CA)). Beads were imaged with a zoom setting of 4.0 through a $60\times$ oil immersion lens with a numerical aperture of 1.4. Stacks of adjacent optical sections separated by 0.5 μm were collected and analyzed. Pixel noise was removed by smoothing the image with a 3×3 kernel (using a coefficient of 4 in the central pixel and 1 in the adjacent pixels) and then thresholding so that only pixels with a value >2 (on a scale of 0–255) were retained (for explanations of image processing techniques used in this paper, see Russ (1995)). Individual beads were followed through as many optical sections as possible before the signal decreased below threshold. Their mean pixel intensity was then measured in each of these optical sections, and the point-spread function was computed.

2.2. Tissue preparation

All animals used in this study were kittens from our breeding colony at the University of California, San Francisco that were 40 days old on the day of sacrifice. On postnatal day 28, geniculocortical axons were labeled by iontophoretic injections of the anterograde neuronal tracer *Phaseolus vulgaris* leucoagglutinin (Pha-L) into the lateral geniculate nucleus. This procedure is described more completely by Antonini and Stryker (1993a). Briefly, brain tissue was fixed by transcardial perfusion with 4% paraformaldehyde, and 70–80 μm sections of primary visual cortex were cut on a vibratome. Axons containing Pha-L were labeled with a polyclonal goat anti-Pha-L antibody (Vector, Burlingame, CA) and visualized with a Cy3 donkey anti-goat IgG secondary antibody (Jackson, West Grove, PA). Synaptophysin was labeled with a monoclonal mouse anti-synaptophysin antibody (Boehringer Mannheim, Indianapolis, IN) followed by a biotinylated horse anti-mouse IgG secondary antibody (Vector). Cy5 labeled egg white avidin (Jackson) allowed visualization of the synaptophysin label. Further details of the immunohistochemical procedures will be presented in a forthcoming paper (Silver and Stryker, in preparation).

Polyclonal rabbit anti-TrkB23 antibodies (raised against amino acid residues 23–36 of the rat TrkB sequence; Yan et al., 1994) and anti-TrkB348 antibodies (raised against amino acid residues 348–363 of the rat TrkB sequence; McCarty and Feinstein, 1998) were obtained from Monte Radeke and Stuart Feinstein and were visualized with a Cy5 donkey anti-rabbit IgG antibody (Jackson). A paper fully describing the use of these anti-TrkB antibodies in kitten primary visual cortex and geniculocortical afferents is also forthcoming (Silver, Radeke, Feinstein, and Stryker, in preparation). Monoclonal mouse anti-GAD65 antibodies (Chang and Gottlieb, 1988) in a GAD-6 hybridoma supernatant were obtained from the Developmental Studies Hybridoma Bank maintained by the Department of Pharmacology and Molecular Sciences, Johns Hopkins University School of Medicine, Baltimore, MD, and the Department of Biological Sciences, University of Iowa, Iowa City, IA, under contract N01-HD-6-2915 from the NICHD.

2.3. Image collection

All confocal images processed for colocalization analysis were collected using a 60 × oil immersion lens with numerical aperture, 1.4; zoom setting, 2.0; aperture setting, 3 (corresponding to an aperture size of 2.16 mm); z-step, 1 μm; and image size, 768 × 512 pixels. This resulted in a pixel size of 0.133 μm. During image collection, the gain and black level microscope values were set so that the full range of pixel intensities was used (0–255) with very little saturation at either end of the intensity range. Excitation filters were used such that when images of Cy3 label were being collected, only the yellow line (568 nm) of the krypton/argon laser illuminated the sample. Similarly, when images of Cy5 label were being collected, only the red line (647 nm) was used for illumination.

2.4. Image processing

All image processing was performed on a Macintosh computer using the public domain NIH Image program (developed at the US National Institutes of Health and available on the Internet at http://rsb.info.nih.gov/nih-image/). The colocalization analysis described in this paper was done with a customized version of NIH Image that is freely available for public use. The program and its documentation can be downloaded from http://phy.ucsf.edu/ ~ idl/colocalization.htm

Most of the descriptions and examples in this paper are taken from tissue labeled with anti-synaptophysin antibodies. For this reason, we refer to the labeled punctate structures as presynaptic sites. However, we found that all of these procedures apply equally well to measurement of colocalization of GAD65- or TrkB-positive punctate structures with labeled axons. Minor differences between the procedure for measuring synaptophysin colocalization and the procedures for measuring GAD65 or TrkB colocalization are mentioned in the text. Otherwise, the term presynaptic site is used to refer generically to a labeled punctate structure for which levels of colocalization with labeled axons are being measured, with synaptophysin serving as the prototypical example.

Based on the computed point spread functions of the fluorescent beads, it was concluded that a distance of 1 μm between adjacent optical sections was sufficient to accurately determine the location of presynaptic sites in three-dimensional space. Because penetration of the anti-synaptophysin antibodies into tissue sections is very poor (Calhoun et al., 1996), the brightest optical section in the stack was designated the reference section (the focal plane of interest) and colocalization within this section was measured by comparison with the optical sections immediately above and below this section. This procedure decreases variability between tissue sections, as images can be collected at the same depth in all tissue sections, thereby normalizing for sources of variability that are dependent on depth such as antibody penetration and the amount of light scattered by the tissue. The brightest optical section was always very close to the top surface of the tissue section.

After the unlabeled cell bodies and blood vessels in the synaptophysin images were traced and masked, the images were thresholded at a level such that the number of pixels above threshold was equal to (total pixels in image-number of cell body and blood vessel pixels)/10. Relative threshold levels higher than this caused some of the more faintly labeled presynaptic sites to fall below threshold, while lower relative threshold levels resulted in poor separation of individual presynaptic sites. Presynaptic sites that formed a contiguous region that was above threshold were segmented from one other using the following procedure: seed pixels were manually placed in the center of each presynaptic site, and an iterative dilation procedure was used to radially expand these seeds until they reached either the edge of the object (as determined by the threshold) or the edge of another expanding seed. In the latter case, the program automatically placed a one-pixel wide boundary between the two expanding seeds. To correct for differences in overall image intensities in adjacent optical sections, the pixel histograms of the sections immediately above and below the reference section were quantitatively matched to the pixel histogram of the reference section.

In the case of the anti-TrkB antibodies, the cell bodies themselves contained punctate label that was difficult to distinguish from the neuropil label. For this reason, pixels within cell bodies and blood vessels were not masked for the TrkB images. The threshold level

for TrkB was set so that the number of pixels above threshold was equal to 2% of the total number of pixels in the image.

2.5. Colocalization analysis

After exclusion of the presynaptic sites located above or below the reference section (Section 3), colocalization analysis was performed. A given presynaptic site was considered to be colocalized with an axon segment if the percentage of pixels contained within the presynaptic site that were also located within axon segment boundaries exceeded a criterion. Also, size criteria were used such that a colocalized object was only included in the final measurement if its size was at least three pixels for synaptophysin and GAD65 and at least two pixels for TrkB. These size criteria were chosen so that the smallest colocalized punctate structures for a given label were included in the colocalization measurements without also including spurious colocalizations due to pixel noise. The colocalization index for a given field was defined as

$$\frac{p}{(a)[s(t/n)]}$$

where p is the total summed intensities of all synaptophysin, GAD65, or TrkB pixels within colocalized presynaptic sites, a is the number of Pha-L-positive pixels within axon segments localized to the reference section, s is the average pixel intensity of the synaptophysin, GAD65, or TrkB label in the entire field following thresholding, t is the total number of pixels in the field, and n is the total number of neuropil pixels in the field (the pixels remaining after the cell bodies and blood vessels have been removed from the analysis).

The rationale for defining the colocalization index in this way is as follows: p represents the total absolute amount of colocalization in the field. However, this value will include many factors that vary from field to field that are not of biological interest. The contribution of these sources of variability to the colocalization index can be removed by including appropriate normalization terms in the index. The a term is the normalization factor for the amount of Pha-L label in the field. Obviously, a field with many labeled axons in it will be likely to have more total colocalization than a field with fewer axons, and this difference should be corrected in the computation of the colocalization index. Similarly, the s term serves to normalize for differences in overall intensity of SVP label across fields. These could be due to differences in quality of perfusion, penetration of antibody, or gain or black level settings on the confocal microscope. The value of the s term will also vary depending on the fraction of the field that consists of neuropil. Since the cell bodies and blood vessels in the non-neuropil portion of the field have no SVP label (and therefore can contain no presynaptic colocalizations), they will decrease the value of s. This decrease is corrected by the t/n term. If the field were to consist of 100% neuropil, n and t would be equal, and the colocalization index would be unchanged. If the field were only 50% neuropil, t/n would have a value of 2, and consequently the s term would be multiplied by a factor of 2 to correct for the fact that only half of the field is being considered for colocalization analysis. In the theoretical limit of a field with 0% neuropil, no colocalizations are possible, and the colocalization index would be mathematically undefined.

2.6. Biological controls

To quantitatively estimate the contribution of out of focus presynaptic sites to the colocalization results, the entire object-based analysis was performed on GAD65 presynaptic sites and Pha-L labeled geniculocortical afferents (see Fig. 5). We considered the colocalization index obtained for these two labels to represent only false positive artifact (noise), while the colocalization index for synaptophysin and Pha-L labeled afferents represents a combination of real colocalizations as well as false positive artifacts (signal + noise). Therefore, the signal-to-noise ratio for the measurement is defined as $(s-g)/g$, where s is the colocalization index for synaptophysin with Pha-L labeled afferents, and g is the colocalization index for GAD65 with Pha-L labeled afferents.

To provide a reference with which to interpret colocalization indices, the amount of colocalization expected based on random overlap of the two labels was computed by performing colocalization analysis on an axon image and a synaptophysin, GAD65, or TrkB image that were collected from different and unrelated parts of a tissue section (although still within portions of primary visual cortex that contained Pha-L labeled geniculocortical axons). This is called the shuffled condition by analogy to electrophysiological cross-correlation studies. Two labels are colocalized above the expected amount due to random overlap when the experimental colocalization index is significantly greater than the shuffled colocalization index. When the experimental value is significantly less than the shuffled value, the two labels are anticolocalized (they coincide less than expected based on random overlap).

2.7. Statistical comparison of object-based and pixel-based analyses

To test the sensitivity of the object-based colocalization analysis used in this paper, a comparison was made with a more conventional pixel-based analysis. Object- and pixel-based analyses were carried out on

identical images for both the experimental and shuffled conditions. This produced a set of colocalization index values for the experimental condition and a separate set for the shuffled condition. If the experimental group and the shuffled group are statistically distinguishable from each other, the amount of colocalization determined by the analysis is significantly different from that based on random overlap of the two labels. Because it is not certain that these data are normally distributed, the non-parametric Mann–Whitney test was used to compare the two groups and a P value of 0.05 was used as the criterion for significance. This statistical comparison between the experimental and the shuffled condition was made for both the pixel-and object-based analyses.

3. Results

3.1. Point spread function

Before collecting colocalization data on tissue sections, it was important to calibrate the confocal microscope and determine the point spread function for a sample consisting of objects of known size. Fluorescent beads of 0.2 μm diameter were imaged using a 60 × oil immersion lens, and the average pixel intensities of individual beads were measured at a series of depths separated by 0.5 μm. The procedure was repeated on the same beads for two different aperture settings on the confocal microscope. Fig. 1 shows the profile of mean pixel intensity relative to the maximum mean intensity of a given bead versus depth in the sample. The width at half-height of this function provides an index of resolution along the z-axis. This measure was 1.74 ± 0.10 μm for an aperture size of 1.67 mm (aperture setting of 2 on the Biorad MRC600 confocal microscope), and it was 1.74 ± 0.07 μm for an aperture size of 2.65 mm (aperture setting of 4). Three conclusions follow from this calibration: (1) under these conditions, resolution in the z-axis is not highly sensitive to aperture setting, (2) even very small particles can show substantial signal in multiple optical sections, and (3) despite this spread of fluorescent signal, comparison of adjacent optical sections spaced 1 μm apart allow the accurate localization of small particles to a single optical section.

3.2. False positive colocalization artifact can contribute substantially to colocalization measurements

The spread of signal across multiple optical sections presents a significant source of false positive artifact in the measurement of colocalization of presynaptic sites and labeled axons, since the diameters of these structures are comparable to the thickness of a single optical section. Fig. 2 indicates an example of this. In this case, a segment of labeled axon and a presynaptic site have overlapping locations in the x–y plane but are separated by approximately 2 μm in the z-axis. Because of the spread of the fluorescent signal, the two appear to be colocalized in the central optical section if the mea-

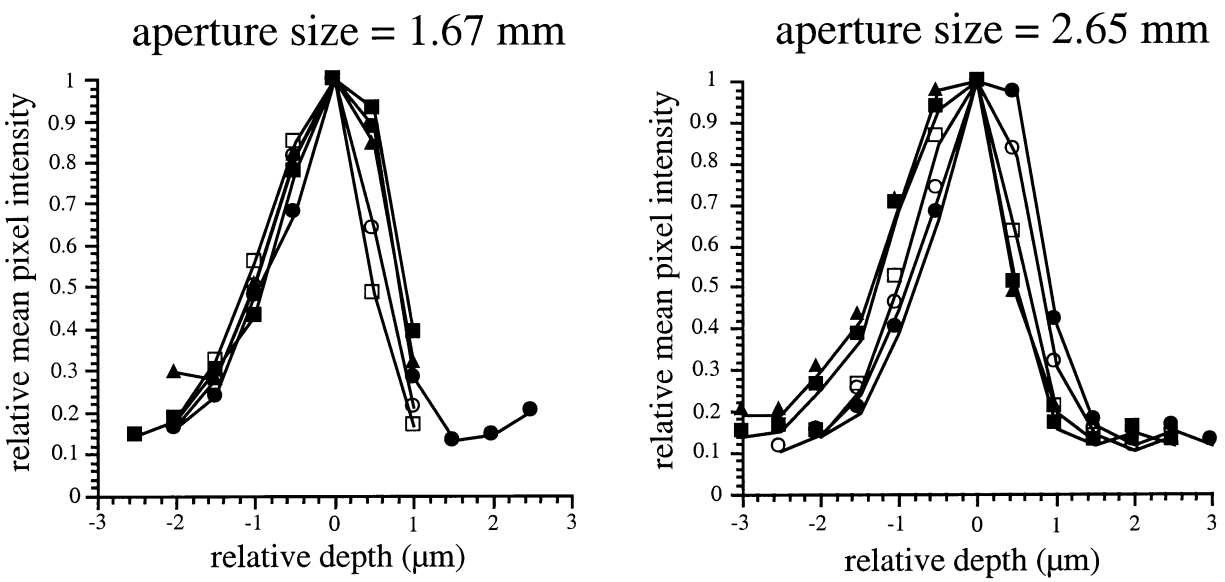

Fig. 1. Spread of fluorescent signal across adjacent optical sections in stacks of confocal images. A total of 0.2 μm fluorescent beads were imaged in a stack of adjacent focal planes separated by 0.5 μm. The average mean pixel intensity of each bead was calculated for every focal plane in which the bead could be detected and then normalized such that the maximum mean pixel intensity was set equal to 1. The focal plane containing the maximum mean pixel intensity for each bead was defined as depth 0 μm, and the other optical sections in the stack were assigned values relative to this central focal plane. This allowed the construction of point spread functions to estimate the spread of fluorescent signal as a function of depth in the sample. The shape of this function can be summarized in a single metric by computing the width at half-height.

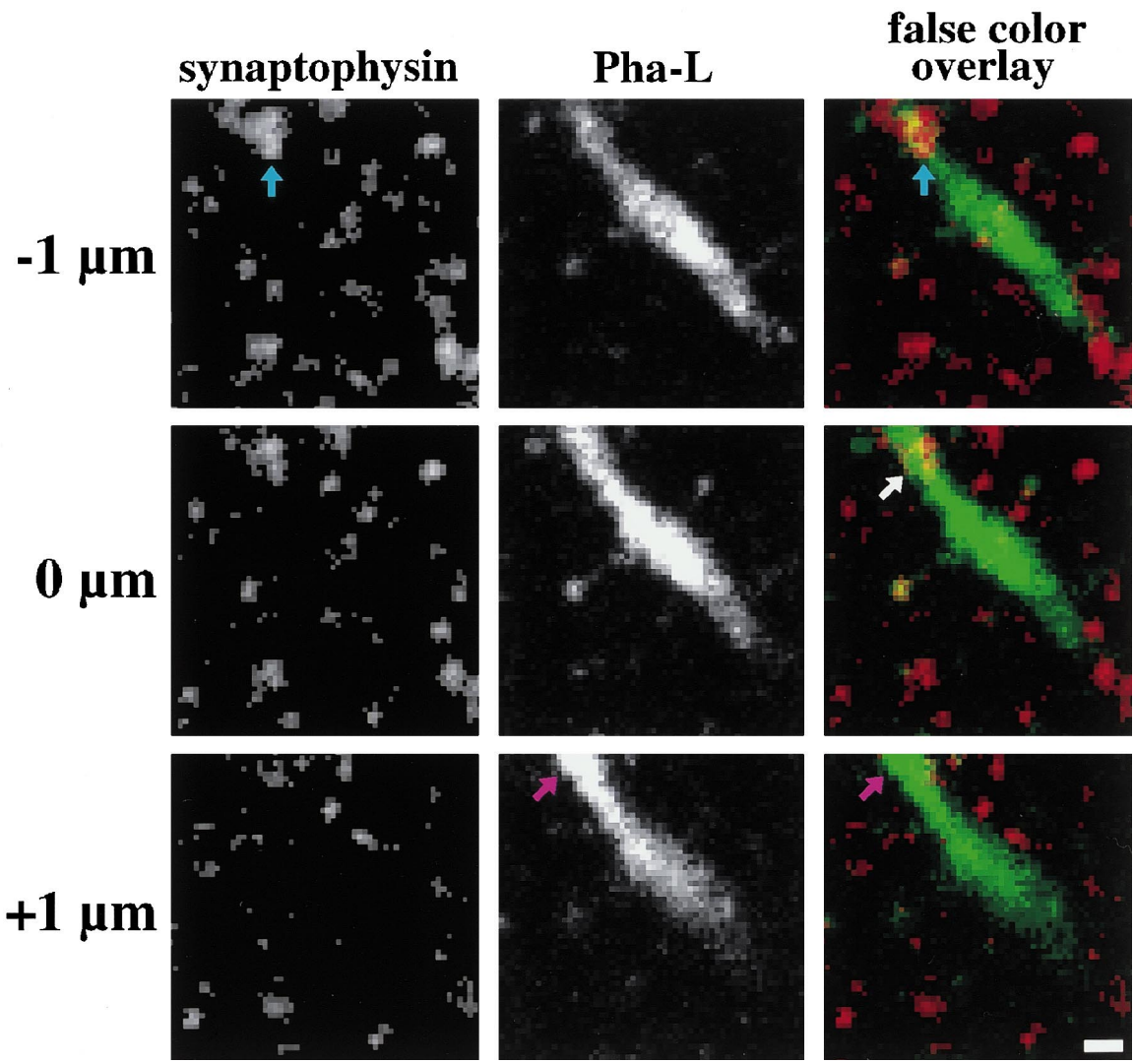

Fig. 2. Spread of fluorescent signal can lead to false positive colocalization artifact. The rows show immunofluorescence from three adjacent optical sections 1 μm apart collected from kitten primary visual cortex. The columns indicate presynaptic sites labeled with synaptophysin, a geniculocortical axon segment labeled with the anterograde neuronal tracer Pha-L, and a false color overlay of the two. In the optical section at top, the blue vertical arrows indicate a presynaptic site that shows more fluorescent signal in the -1 μm optical section than it does in the 0 μm optical section, suggesting that its true location in depth is in the -1 μm section. In the optical section at bottom, the portion of the axon segment corresponding to the x–y location of this presynaptic site is indicated by the purple diagonal arrows. This portion of the axon segment shows maximal fluorescent signal in the $+1$ μm optical section, suggesting that its location in depth is in the $+1$ μm optical section. The white arrow in the middle optical section shows the false positive colocalization of the presynaptic site and axon segment that would have been considered an actual colocalization if only the central optical section images had been analyzed and no comparisons had been made between adjacent optical sections. Scale bar, 1 μm.

sure of colocalization is the number or summed intensities of yellow pixels in the false color overlay. However, if the cluster of SVP label and the segment of labeled axon are treated as objects with well-defined boundaries, they can then be localized in three-dimensional space. In this way, more accurate colocalization is possible.

The methods used here for defining the boundaries of labeled axons and clusters of SVP labeling differ. For axons, the optical section of interest (the reference section) is manually compared to optical sections immediately above and below to determine which portion of each labeled axon branch is brighter in the reference section than in the optical section either above or below. The boundaries of these axon segments are traced by hand, and the image is binarized.

For presynaptic sites, the clusters of SVP label are first segmented from each other in the reference section. This is accomplished by thresholding the image such that the brightest 10% of the pixels in the neuropil retain their values and all other pixels are set to 0. The choice of this method versus a method that uses an

absolute threshold level allows for normalization of several sources of fluorescent signal variability from field to field including, but not limited to, quality of perfusion of the animal, amount of antibody penetration, differences in gain and black level microscope settings, and amount of tissue photobleaching. Before any thresholding can occur, the pixels located in the neuropil must be identified and separated from those within cell bodies and blood vessels. Because there is no SVP label inside of cell bodies or blood vessels, these pixels should be excluded from further colocalization analysis (see Section 2 for details). The boundaries of the cell bodies and blood vessels are traced by hand, and all of the pixels within and including the boundaries are masked and removed from further analysis. The remaining neuropil pixels are then thresholded.

3.3. Thresholding and segmentation allow presynaptic sites to be analyzed as objects instead of sets of pixels

Although thresholding creates well defined boundaries for many of the presynaptic sites, sometimes neighboring clusters of SVP label are above threshold and form one contiguous object (Fig. 3). For colocalization analysis to be accurate, these presynaptic sites should be segmented from each other and analyzed independently. This is accomplished by manually indicating the pixel that is closest to the center of each presynaptic site. These seed pixels become the centers of expanding rings which continue expanding until they either reach a presynaptic site edge defined by the threshold operation or until they encounter another expanding ring. In the latter case, a one-pixel wide boundary is created between the two contiguous presynaptic sites, thereby effectively segmenting them.

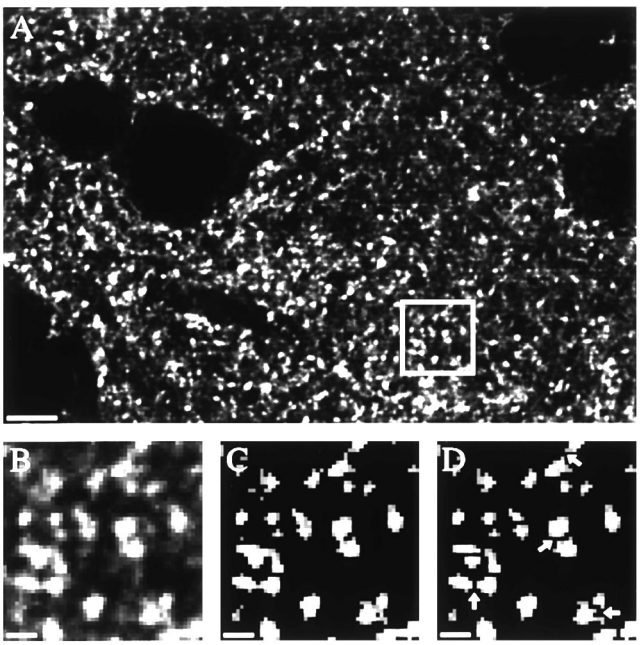

Fig. 3. Image thresholding and segmentation allows separation of individual clusters of SVP label for further object-based analysis. (A) Low power raw image of synaptophysin immunofluorescence. Punctate labeling of presynaptic sites is present in the neuropil, and staining is absent from cell somata. Box indicates the portion of the image used for image processing (B)–(D). (B). Higher power view of the boxed region in (A). (C) The same image shown in (B) thresholded such that the brightest 10% of the pixels in the field retained their intensity values and all other pixels were set to a value of 0. (D) Segmentation of individual presynaptic sites following placement of seed pixels and subsequent iterative dilation (see Section 2 for details). Arrows indicate the one pixel wide boundary used to segment contiguous clusters of SVP label. Scale bar: 5 μm in A, 1 μm in (B)–(D).

3.4. Colocalization in three dimensions

To determine the location of segmented presynaptic sites along the z-axis, it is necessary to compare pixel intensity values in adjacent optical sections. This comparison is only meaningful if the average intensity of neuropil SVP label is equivalent in the optical sections that are being compared. Unfortunately, equivalence is rarely the case, because optical sections that are nearer the surface of the tissue section are subject to less light scattering and typically have better antibody penetration than deeper optical sections. To correct for these overall changes in SVP label as a function of depth, the pixel intensity histograms of the optical sections immediately above and below the reference section are matched to the reference section histogram. Histogram matching refers to an image processing algorithm that does not change the rank ordering of pixel intensity values in an image but simply reassigns the values to match some other distribution. This matching procedure is a valid correction only under the assumption that the true distributions of the labeled objects are similar throughout the series of optical sections under consideration. This assumption is correct in the case of synaptic vesicle clusters, but it may not be correct in other circumstances.

After the match histogram procedure is complete, each cluster of SVP is classified either as: (1) a presynaptic site truly located in the reference section, or (2) a presynaptic site located in a section above or below the reference section and contributing out of focus scatter to the reference section. This is accomplished by defining the set of x–y pixel coordinates contained within the presynaptic site in the reference section and then comparing the mean intensity values of this set of pixels to the set of pixels in the same x–y locations in the optical sections immediately above and below the reference section.

Whether a given presynaptic site in the reference section is colocalized with a segment of labeled axon in

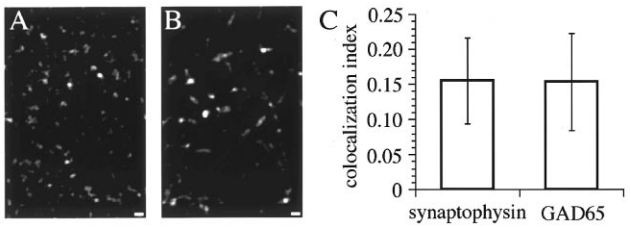

Fig. 4. The overall spatial statistics of synaptophysin and GAD65 immunofluorescence are similar, thereby allowing quantitative comparison of their colocalization indices. (A) Thresholded synaptophysin immunofluorescence. (B) Thresholded GAD65 immunofluorescence. The patterns of synaptophysin and GAD65 label consist of punctate structures of approximately the same size distribution and density. Scale bars: 1 μm. (C) Colocalization indices of synaptophysin and GAD65 with Pha-L labeled geniculocortical axons in the shuffled condition (see Section 2). Synaptophysin or GAD65 images collected in one part of the tissue section were colocalized with Pha-L axon images collected in either a different unrelated region of the same section or in a different section entirely ($n = 6$ pairs of images). The resulting colocalization indices give an estimate of the amount of colocalization expected based on random overlap of either synaptophysin or GAD65 with the Pha-L label. Two presynaptic labels with similar spatial statistics should give similar colocalization indices when colocalized with axons in the shuffled condition, although of course their actual colocalization indices in the experimental condition could be quite different from one another when carried out on pairs of images collected from the same field.

the same plane depends on the amount of overlap of the two objects. Given that fluorescent images of objects have some spread both in the x–y plane and along the z-axis, the relationship between the physical boundaries of the object and the boundaries of the fluorescent image of the object is not known quantitatively and is difficult to determine with precision. To address this issue, a quantitative estimate of the incidence of false positive artifactual colocalizations for a range of different colocalization stringencies was needed.

To determine colocalization, thalamic afferents projecting to layer IV of P40 kitten primary visual cortex were labeled with the anterograde neuronal tracer *Phaseolus vulgaris* leucoagglutinin (Pha-L). The Pha-L was visualized with an anti-Pha-L antibody, and presynaptic sites were labeled with an anti-synaptophysin antibody. To estimate the amount of false positive artifact due to out of focus presynaptic sites, a control antibody against GAD65 was used. GAD65 is an isoform of glutamic acid decarboxylase that is localized primarily to presynaptic terminals of GABAergic inhibitory neurons (Kaufman et al., 1991; Esclapez et al., 1994). Because the geniculocortical afferents make only asymmetric (and therefore excitatory) synapses (Garey and Powell, 1971; Freund et al., 1985), any apparent colocalization between GAD65-positive presynaptic sites and Pha-L-positive geniculocortical afferents is considered to be false positive colocalization artifact. Since the spatial statistics of synaptophysin labeling and GAD65 are similar in our images (Fig. 4), it is appropriate to quantitatively compare the colocalization indices obtained for synaptophysin and Pha-L labeled axons with those from GAD65 and Pha-L labeled axons.

3.5. Effects of varying colocalization stringency

Since all apparent GAD65 colocalizations are artifactual, they can be considered noise in the measurement, while synaptophysin colocalizations will presumably be a combination of this noise and actual colocalizations (signal). Therefore, a signal-to-noise ratio for colocalization analysis can be computed for a variety of colocalization stringencies. In this case, colocalization stringency is a threshold value of the percentage of pixels in an individual presynaptic site that are also located within the boundaries of a labeled axon segment. For each presynaptic site, this percentage must exceed the stringency criterion to be counted as colocalized with the labeled axon segment.

Fig. 5 demonstrates that as the colocalization criterion is made more stringent, the colocalization index decreases for both synaptophysin and GAD65. However, the relative size of this decrease is greater for GAD65 than it is for synaptophysin, indicating that increasing the stringency has the effect of selectively removing the contribution of false positive colocalizations to the colocalization index. That is, although some genuine colocalizations are excluded by making the colocalization criterion stricter, many more false positive colocalizations are excluded in the process. This is also demonstrated by the signal-to-noise ratio measurements which indicate that the signal-to-noise ratio continues to increase up to a colocalization stringency of 100% (Fig. 5).

3.6. Object-based colocalization analysis is more reliable and more sensitive than pixel-based analysis

Although the object-based colocalization analysis presented so far shows that the method can correctly discriminate a presynaptic marker that is colocalized with labeled geniculocortical axons (synaptophysin) from one that is anticolocalized with the same population of axons (GAD65), the necessity of using an object-based analysis to accomplish this rather than a pixel-based one has not been demonstrated. To show this, the colocalization analysis was carried out on Pha-L labeled geniculocortical afferents and an antibody raised against a portion of the high affinity neurotrophin receptor (anti-TrkB23). A direct comparison of pixel-based and object-based colocalization analyses of the same raw images was made. The differences between the two analyses were that the pixel-based analysis did not include segmentation of the label into

objects, comparison of adjacent optical sections for determining the location of the labeled structures in three dimensions, or a size criterion for colocalization. Otherwise, the two analyses were identical, including the tracing of axon segments located within the focal plane of interest and the use of the colocalization index defined in Section 2.5. Fig. 6 clearly shows that the object-based analysis excludes false positive colocalization artifacts which are present in the pixel-based analysis.

To quantify these differences, the computed colocalization indices for pixel-based and object-based analyses were compared to the amount of colocalization that would be expected based on random overlap of the Pha-L and TrkB23 labels (the shuffled condition, see Section 2 for details). Although the pixel-based analysis suggests that the amount of colocalization of TrkB23 with labeled geniculocortical axons is not significantly different from the expected amount of colocalization

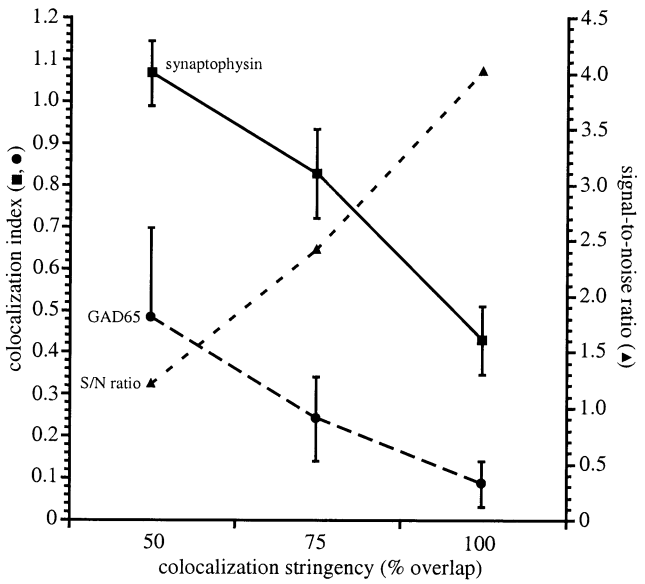

Fig. 5. Synaptophysin immunofluorescence is significantly more colocalized with Pha-L-labeled geniculocortical axons than is GAD65 immunofluorescence with the same population of axons, and the difference between synaptophysin and GAD65 becomes greater with increasing colocalization stringency. Colocalization stringency is defined as the minimum percentage of pixels in a cluster of antigen label that must overlap with a labeled axon in order to be considered colocalized. Since the amount of actual colocalization of the GAD65 antigen and the geniculocortical axons is 0, any apparent colocalization of these two labels is defined as noise (false positive colocalization artifact) in the measurement. The apparent colocalization index for synaptophysin is considered to be a combination of this noise and real colocalizations (signal). Therefore, the 'signal-to-noise ratio' is computed as the difference in the colocalization indices for synaptophysin and GAD65 divided by the colocalization index for GAD65 (see Section 2). For all colocalization stringencies examined, the colocalization index for synaptophysin (squares) is greater than that of GAD65 (circles). In addition, the signal-to-noise ratio (triangles) increases as the colocalization stringency increases ($n = 6$ pairs of images). This indicates that while increasing colocalization stringency decreases both signal and noise, proportionately more noise than signal is removed, resulting in a more sensitive and accurate measure of colocalization. Note that it is appropriate to compare quantitatively the colocalization indices for synaptophysin and GAD65 because the spatial statistics of the two labels are so similar (see Fig. 4).

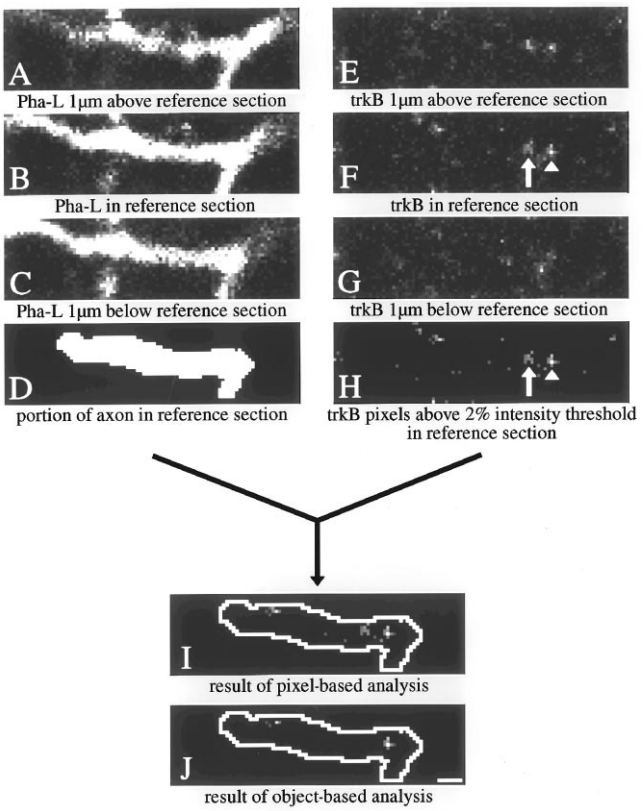

Fig. 6. The use of object-based analysis removes much of the false positive colocalization artifact that is present with pixel-based analysis. (A)–(C) A stack of three adjacent optical sections showing Pha-L immunofluorescence from a labeled geniculocortical axon segment in kitten primary visual cortex. (D) Binarized portion of the axon that is located in the reference section. Adjacent portions of the axon segment located above and below the reference section have been eliminated from further analysis. (E)–(G) TrkB348 immunofluorescence from the same stack of optical sections shown in (A)–(C). The arrow in (F) indicates a potential source of false positive colocalization artifact from a TrkB348 positive punctate structure that produces signal in the reference section but is actually located in the optical section 1 μm above the reference section. The arrowhead in (F) indicates a TrkB348 positive punctate structure that is actually located in the reference section. (H) (F) Following intensity thresholding. Only those pixels that make up the 2% of the brightest pixels in (F) are shown. Arrow and arrowhead are as in (F). (I) Result of pixel-based analysis. This is a simple overlay of those pixels in (D) and (H) that lie within the binarized axon segment. This pixel-based analysis fails to exclude the false positive colocalization artifact. As a result, the colocalization signal has a substantial amount of artifactual noise. (J) Result of object-based analysis. Each segmented object in (H) is treated as a separate set of pixels which must meet a size criterion (2 pixels in this case). An object is only considered to be colocalized if it is located entirely within the boundaries of the binarized axon segment and if it has more signal in the reference section than in either the optical section 1 μm above or 1 μm below. With this object-based method, the false positive colocalization artifact is excluded. Scale bar: 1 μm.

based on random overlap of the two labels ($P > 0.5$, Mann–Whitney test), the object-based analysis produces a colocalization index that is significantly greater than random levels of colocalization ($P < 0.05$, Mann–Whitney test). In addition to demonstrating that the object-based analysis is significantly more sensitive than the pixel-based analysis in this case, this example also shows that the colocalization method presented here can be used to determine whether a given antigen of unknown subcellular distribution is expressed on an axon population of interest as well as being used to measure the density of presynaptic sites in labeled axons.

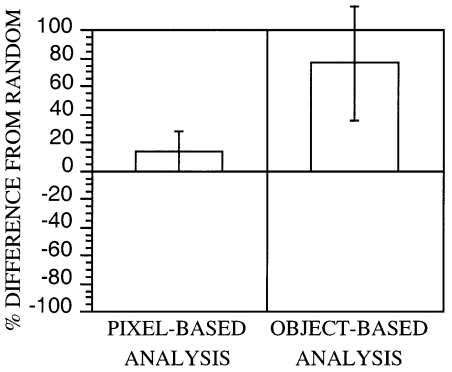

Fig. 7. Quantification of the differences between pixel-based and object-based analyses. Twelve pairs of immunofluorescence images of Pha-L labeled geniculocortical axons and TrkB23 antigen from kitten primary visual cortex of two animals were analyzed using the pixel-based and object-based methods. A colocalization stringency of 100% was used for the object-based analysis. For the two labels, the expected amount of colocalization based on random overlap was estimated by carrying out the colocalization analysis in the shuffled condition. Percent difference from random was calculated by subtracting the colocalization index in the shuffled condition from the colocalization index in the experimental condition and then dividing by the colocalization index in the shuffled condition. Therefore, a value of 0 indicates that the amount of colocalization is equal to that expected based on random overlap. Positive values indicate colocalization of the two labels, and negative values suggest that the two labels are anticolocalized. Error bars show the S.E.D., which is the square root of the sum of the squares of the S.E.M. for the experimental and shuffled conditions. The pixel-based analysis produces a result that is not significantly different from the amount of colocalization expected based on random overlap of the two labels ($P > 0.5$, Mann–Whitney test). It is therefore unable to determine whether the TrkB23 antigen is localized to geniculocortical axons, presumably because the measurement is dominated by false positive colocalization artifact. Object-based analysis, on the other hand, shows an amount of colocalization significantly greater than that expected based on random overlap ($P < 0.05$, Mann–Whitney test) and therefore clearly indicates that the TrkB23 antigen is expressed in geniculocortical axons.

4. Discussion

We have presented an object-based method for measuring the amount of colocalization of immunofluorescently labeled antigens with a population of axons that are labeled with an anatomical tracer. If the antigen is a synaptic vesicle protein or other marker of presynaptic terminals, the method can be used to quantitatively measure relative densities of presynaptic sites within axons of interest. The density of label can be expressed as either the number of clusters of SVP label per unit length of labeled axon or the total amount of SVP label per unit length of labeled axon. These measures are useful for characterizing changes in density or distribution of presynaptic sites during development or plasticity (Silver and Stryker, in preparation).

For other antigens for which the subcellular distribution is not completely characterized, the colocalization method described here can be used to determine whether the amount of colocalization of the antigen with the axons of interest is significantly greater than or less than the amount of colocalization expected based on random overlap of the two labels. Although a measured colocalization index that is not significantly different from the amount expected based on random overlap is an indeterminate result with respect to whether than antigen is colocalized with the axons of interest, a result in which the colocalization index is significantly greater than the random levels is clear evidence for absolute colocalization and provides a relative measure of the amount of this colocalization.

While the examples presented in this paper stress the advantages of object-based colocalization over a pixel-based approach, for many applications the differences between the two methods are not substantial. In preparations where the three-dimensional location of the antigens and axons are known precisely, the two methods are equally valid. This would be the case for most colocalization analyses using cell cultures. Additionally, if the pattern of expression of the antigen of interest is not punctate but instead labels structures much larger than the width of the optical section, an object-based analysis is not appropriate, since the objects cannot be definitively localized to a single focal plane. This situation may arise if the antigen is expressed throughout the cell or continuously throughout the entire axonal arbor of a neuron. In this case, providing the label is not too dense, the three-dimensional shape of the label should allow for an accurate determination of colocalization.

The object-based analysis is particularly well suited for applications in which the antigen of interest labels punctate structures whose size is equal to or less than the thickness of the optical section. An object-based approach becomes essential if there is a substantial amount of labeling of the antigen of interest in neuropil structures that are located in the area of projection of the labeled axons of interest. These could include dendrites, other axons, or glia. The possibility of substantial false positive colocalization artifact is proportional to the amount of antigen label in these structures, and

pixel-based analyses cannot reliably distinguish true colocalization from the apparent colocalization observed when a labeled punctate structure is located in the focal plane just above or just below the labeled axon (see Figs. 2, 6 and 7).

Given that most injections of anterograde neuronal tracers label a relatively small number of cells, the portion of the neuropil volume in the area of projection that is actually occupied by labeled axons will typically be very small. Therefore, even if the probability of incorrectly categorizing an individual apparent (false positive) colocalization as an actual colocalization can be very low, the fact that the pool of potential artifactual colocalizations will typically be substantially larger than the pool of actual colocalizations means that the amount of false positive colocalization artifact in an entire field can be very high if steps are not taken to reduce it. As we have demonstrated here, the object-based colocalization analysis effectively separates actual colocalizations from false positive artifactual colocalizations and thereby provides a reliable and accurate measure of colocalization of a given antigen of interest with a population of labeled axons.

Acknowledgements

Michael A. Silver was a Howard Hughes Medical Institute Predoctoral Fellow. This work was supported by NIH grant EY02874 to Michael P. Stryker. The authors would like to thank Monte Radeke and Stuart Feinstein for generously providing anti-TrkB polyclonal antibodies and Antonella Antonini and Christopher Trepel for discussion of the manuscript. M.A.S. would like to thank Antonella Antonini for teaching me many of the techniques used in this paper and for being a wonderful mentor.

References

Antonini A, Stryker MP. Development of individual geniculocortical arbors in cat striate cortex and effects of binocular impulse blockade. J Neurosci 1993a;13:3549–73.

Antonini A, Stryker MP. Rapid remodeling of axonal arbors in the visual cortex. Science 1993b;260:1819–21.

Calhoun ME, Jucker M, Martin LJ, Thinakaran G, Price DL, Mouton PR. Comparative evaluation of synaptophysin-based methods for quantification of synapses. J Neurocytol 1996;25:821–8.

Carrington WA, Fogarty KE, Lifschitz L, Fay FS. Three-dimensional imaging on confocal and wide-field microscopes. In: Pawley JB, editor. Handbook of Biological Confocal Microscopy, revised edition. New York: Plenum, 1990:151–61.

Chang Y-C, Gottlieb DI. Characterization of the proteins purified with monoclonal antibodies to glutamic acid decarboxylase. J Neurosci 1988;8:2123–30.

Esclapez M, Tillakaratne NJK, Kaufman DL, Tobin AJ, Houser CR. Comparative localization of two forms of glutamic acid decarboxylase and their mRNAs in rat brain supports the concept of functional differences between the forms. J Neurosci 1994;14:1834–55.

Freund TF, Martin KAC, Whitteridge D. Innervation of cat visual areas 17 and 18 by physiologically identified X- and Y-type thalamic afferents. I. Arborization patterns and quantitative distribution of postsynaptic elements. J Comp Neurol 1985;242:263–74.

Friedlander MJ, Martin KA, Wassenhove-McCarthy D. Effects of monocular visual deprivation on geniculocortical innervation of area 18 in cat. J Neurosci 1991;11:3268–88.

Garey LJ, Powell TPS. An experimental study of the termination of the lateral geniculo-cortical pathway in the cat and monkey. Proc R Soc London B 1971;179:41–63.

Hamos JE, Van Horn SC, Raczkowski D, Sherman SM. Synaptic circuits involving an individual retinogeniculate axon in the cat. J Comp Neurol 1987;259:165–1692.

Hooper JE, Carlson SS, Kelly RB. Antibodies to synaptic vesicles purified from *Narcine* electric organ bind a subclass of mammalian nerve terminals. J Cell Biol 1980;87:104–13.

Humphrey AL, Sur M, Uhlrick DJ, Sherman SM. Projection patterns of individual X- and Y-cell axons from the lateral geniculate nucleus to cortical area 17 in the cat. J Comp Neurol 1985;223:159–89.

Kaufman DL, Houser CR, Tobin AJ. Two forms of the gamma-aminobutyric acid synthetic enzyme glutatmate decarboxylase have distinct intraneuronal distributions and cofactor interactions. J Neurochem 1991;56:720–3.

LeVay S, Stryker MP. The development of ocular dominance columns in the cat. In: Ferrendelli JA, editor. Society for Neuroscience Symposia: Aspects of Developmental Neurobiology, vol. 4. Bethesda, MD: Society for Neuroscience, 1979:83–98.

Matthew WD, Tsavaler L, Reichardt LF. Identification of a synaptic vesicle-specific membrane protein with a wide distribution in neuronal and neurosecretory tissue. J Cell Biol 1981;91:257–69.

McCarty JH, Feinstein SC. Activation loop tyrosines contribute varying roles to TrkB autophosphorylation and signal transduction. Oncogene 1998;16:1691–700.

Pinches EM, Cline HT. Distribution of synaptic vesicle proteins within single retinotectal axons of *Xenopus* tadpoles. J Neurobiol 1998;35:426–34.

Russ J. The Image Processing Handbook, 2nd edition. Boca Raton, FL: CRC Press, 1995.

Südhof TC. The synaptic vesicle cycle: a cascade of protein–protein interactions. Nature 1995;375:645–53.

Wiedenmann B, Franke WW. Identification and localization of synaptophysin, an integral membrane glycoprotein of M_r 38,000 characteristic of presynaptic vesicles. Cell 1985;41:1017–28.

Yan Q, Matheson C, Sun J, Radeke MJ, Feinstein SC, Miller JA. Distribution of intracerebral ventricularly administered neurotrophins in rat brain and its correlation with Trk receptor expression. Exp Neurol 1994;127:23–36.